International Journal of Science and Research (IJSR)
ISSN (Online): 2319-7064
Index Copernicus Value (2013): 6.14 | Impact Factor (2015): 6.391

An Isolated Single Switch PV Integrated DC–DC Converter

Rinu M P[1], Veena Wilson[2]

[1]M. Tech Student, Department of EEE, FISAT , Angamaly, Kerala – 683577, India

[2]Assistant Professor, Department of EEE, FISAT, Angamaly, Kerala – 683577, India

Abstract: ***Isolated converters are desirable in the DC-DC power conversion applications where isolation or a large voltage step-up gain is needed. Traditional isolated DC-DC converters either utilize many switches to achieve high efficiency or use few switches which result in low efficiency. The high switching frequencies in power converters further increases the switching losses, and electromagnetic interferences. These losses can be overcome by employing soft switching techniques. In this paper a new single-switch isolated DC-DC converter is introduced for voltage regulation in solar photovoltaic (PV) system. The presented converter is able to offer low cost and high power density in step-up applications. The modified DC-DC converter has the advantage of using less number of switches than other existing isolated DC-DC converters. Low rated lossless snubber used in the modified topology can reduce the transformer volume due to low magnetizing current. Efficiency of the PV panel can be improved by employing MPPT alogorithm. Simulation studies are carried out in MATLAB to verify the theoretical analysis and show that the modified converter is effective for PV systems. Experimental results further validate the simulation studies.***

Keywords: Isolated step up dc-dc converter, single switch, ZVS switching, ZCS switching, MPPT

1. Introduction

The limited availability of energy sources has become an inevitable global problem. Therefore we are looking for renewable energy sources instead of non re newable energy sources. Solar energy is the most exploited source of renewable energy. As the terminal voltage of solar module is very low, a DC-DC converter is essential for the useful utilization of energy. Several methods exist to achieve

DC-DC voltage conversion. Each of these methods has its specific benefits and disadvantages, depending on a number of operating conditions and specifications. Examples of such specifications are the voltage conversion ratio range, the maximal output power, power conversion efficiency, number of components, power density, galvanic separation of input and output, etc. When designing fully- integrated DC-DC converters these specifications generally remain relevant. A

DC-DC converter is normally chosen because of its high efficiency in converting the input power to output power. Many conventional DC-DC converters are present in which isolated converters are preferred because the non-isolated converters do not satisfy the requirements of galvanic isolation standards.[1]-[3]. In many DC-DC applications, multiple outputs are required and output isolation may need to be implemented depending on the application. In addition, input to output isolation may be required to meet safety specification. The electrical isolation in switching DC power supplies are provided by high frequency isolation transformer.[4] But the voltage stresses on the transformer winding and output diode are very high in the conventional isolated converters such as flyback converter, forward converter, push-pull converter, and full-bridge converter. The high voltage stress on the switches results in usage of components having high power handling capability, which in turn increases the cost.[5]. Snubber circuits are normally used for reducing the switch voltage stress. The snubber circuit again decreases the converter efficiency by dissipating energy in it[6][7]. A non-dissipative snubber can be implemented by using only capacitor and an inductor and it can be utilized to reduce the voltage stress. Also the converter efficiency will be increased because of the recovery of energy trapped in the leakage inductor.[8]

The main aim of this project is to develop a PV integrated single switch isolated dc-dc converter that can produce a high voltage dc as the output. The voltage stress on the switch can be reduced along with high conversion efficiency by implementing a non-dissipative snubber circuit. The overall system size can be minimized and the overall efficiency can also be improved. The rating of power electronics components can be reduced in order to reduce the cost. The modified topology can maintain a constant output voltage irrespective of input voltage variations with closed loop feedback.

2. Single Switch Isolated DC-DC Converter

The Fig 2.1 shows the circuit diagram of single switch isolated ZVS-ZCS converter. Converter includes a input filter L_i, switch S_1, a lossless snubber consisting of capacitor C_s , inductor Ls, and diodes D_{S1}, D_{S2} and clamp capacitor C_c in the primary side. In the secondary side L_r, C_r forms series resonant circuit and with diodes D_1 and D_2. The lossless snubber circuit with L_s, C_s resonates which tranverses the voltage across the switch from zero to its peak and back down to zero , at this point switch is activated. Thus ZVS is achieved. Similarly in the secondary side of transformer L_r, C_r resonates to tranverse the energy thus ZCS can be achieved to turn off the diodes.

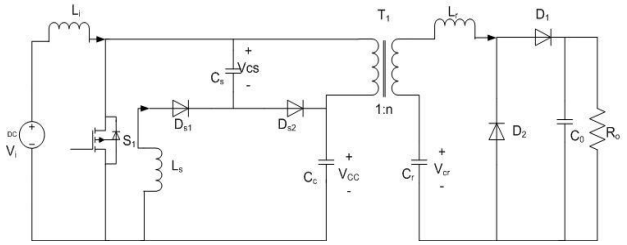

Figure 2.1: Isolated single switch ZVS-ZCS Converter

A. Operating Principle

The input filter and magnetizing inductance are assumed to be large so that they can be teated as constant current sources during the switching period. Output capacitance and clamp capacitance are also assumed as large so that they can be considered as constant voltage sources. Thus V_{cc} is treated same as the input voltage. Figure 2.2 shows the theoretical waveforms of the converter.

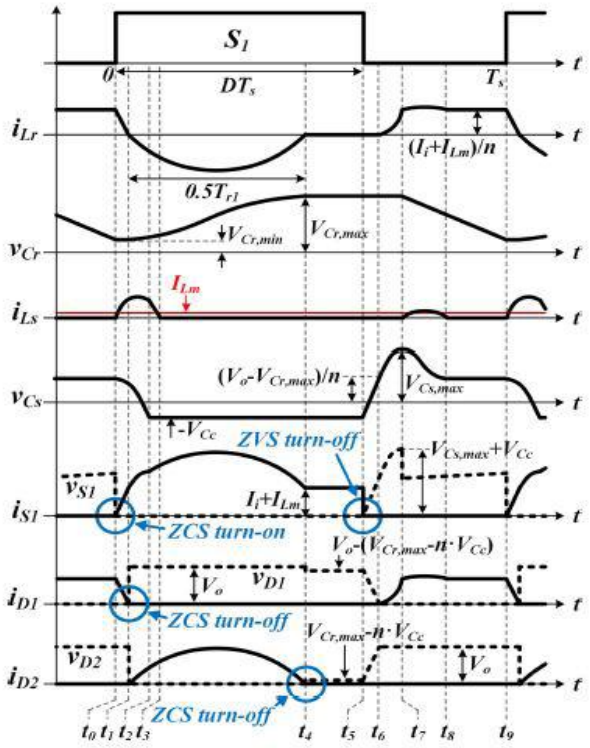

Figure 2.2: Key waveforms of the converter

B. Modes of Operation

Nine modes of operation exist within T_s.

MODE 1 (t_0 - t_1) : This mode begins when switch S_1 is turned ON. Equivalent circuit of this mode is shown in Fig.2.3. L_s and C_s start resonating and resonant current i_{Ls} flows through L_s , D_{s1} , C_s and S_1. Since induced voltage $_{VCr;min}$ - nV_{Cc}- V_0 across L_r makes time interval from t_0 to t_1 very short, current i_{Lr} appears to decrease almost linearly. Current through S_1 increases with the slope of i_{Lr} , resulting in ZCS turn-on of S_1 . The turn-on loss of switch associated with energy stored in MOSFET's output capacitance is negligible in this low input voltage application. This mode ends when current i_{Lr} reaches 0 A. It is noted that diode D_1 is turned OFF under ZCS condition.

MODE 2 (t_1 – t_2) : This mode begins when current i_{Lr} changes its direction. Equivalent circuit of this mode is shown in Fig.3.5. L_r and C_r start resonating and resonant current i_{Lr} ows through L_r ,C_r and D_2. When voltage across snubber capacitor C_s equals V_{Cc}, L_s - C_s resonance ends.

MODE 3 (t_2 – t_3) : This mode begins when diode D_{s2} is turned ON. When current i_{Ls} reaches 0A this mode ends. It is noted that diodes D_{s1} and D_{s2} are turned OFF under ZCS condition.

MODE 4 (t_3 – t_4) : The $_{Lr}$ - C_r resonance keeps on during this mode and ends when current i_{Lr} reaches 0A. Equivalent circuit of this mode is shown in fig.2.3. Diode D_2 is turned OFF under ZCS condition.

MODE 5 (t_4 – t_5) : During this mode, a constant current flows through S_1 whose value is the sum of the input current I_i and the magnetizing current I_{Lm}. Fig.2.3 shows equivalent circuit of this mode of operation.

MODE 6 (t_5 – t_6) : The mode begins when S_1 is turned OFF. Then, I_i + I_{Lm} flows through C_s ,D_{s2} and Cc. Voltage across snubber capacitor C_s increases linearly with the slope of (I_i + I_{Lm})/C_s, resulting in ZVS turn-off of S_1. This mode ends when v_{Cs} becomes equal to (V_0 - $V_{Cr;max}$)/n.

MODE 7 (t_6 – t_7) : This mode begins when diode D_1 is turned ON. Equivalent circuit of this mode is shown in Fig.2.3. L_r and C_s start resonating and resonant current i_{Lr} flows through C_s ,D_{s2} ,L_r ,D_1 and C_r. Assuming that C_s >> n^2Cr, vCr can be considered constant and resonance frequency ω_{r3} can be determined by C_s and L_r as ω_{r3} = n/$\sqrt{L_rC_s}$. This mode ends when current i_{Lr} becomes equal to (I_i + I_{Lm})/n.

MODE 8 (t_7 – t_8) : This mode begins when diode D_{s1} is turned ON. Equivalent circuit of this mode is shown in Fig.2.3. Ls, Cs, Lr and Cr start resonating and resonant current i_{Lr} flows through Ls, D_{s1} ,Cs ,Cc ,Lr ,D_1 , and Cr. This mode ends when current i_{Ls} reaches 0 A.

MODE 1 (t0 – t1):

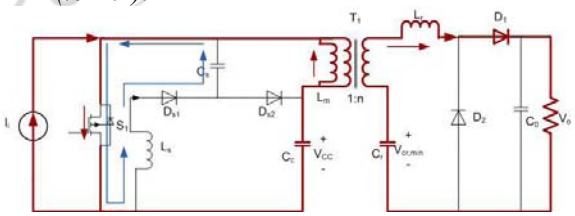

MODE 2 (t1 – t2):

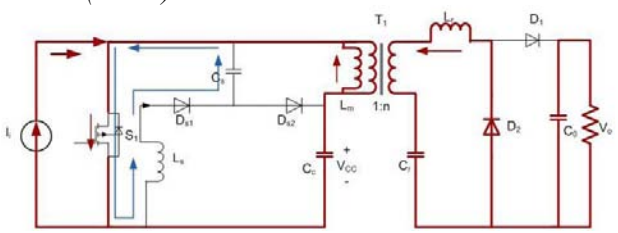

MODE 3 (t2 – t3):

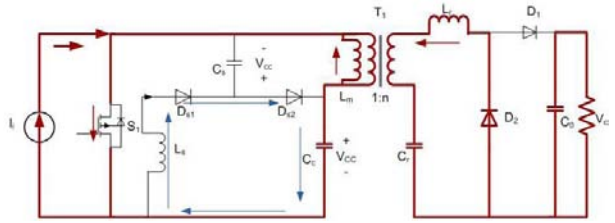

MODE 4 (t3 – t4) :

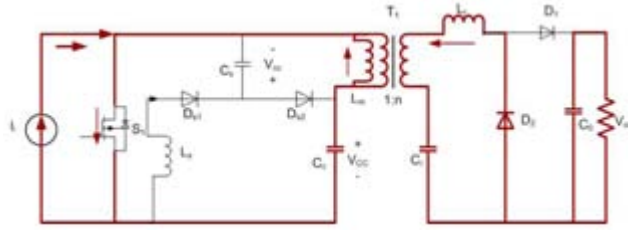

MODE 5 (t4 – t5) :

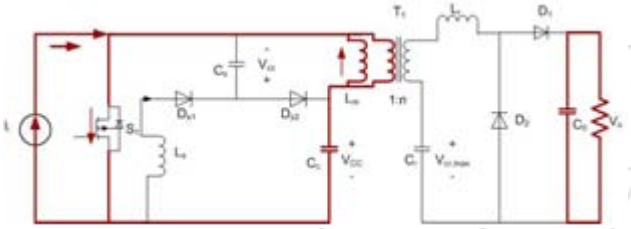

MODE 6 (t5 – t6) :

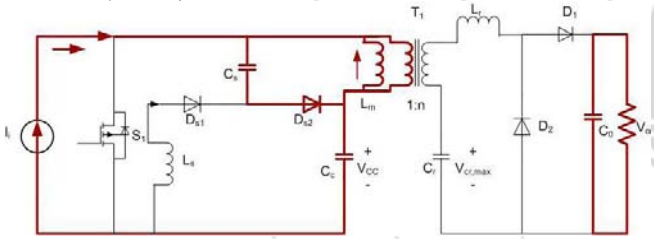

MODE 7 (t6 – t 7) :

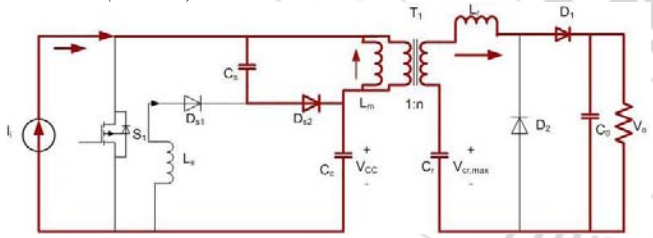

MODE 8 (t7 – t8) :

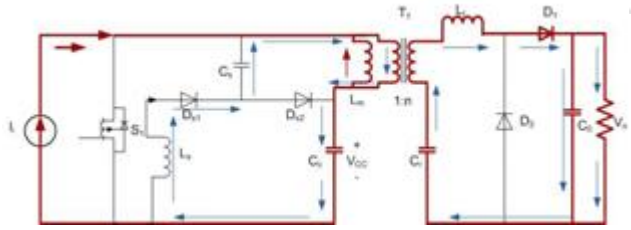

MODE 9 (t8 – t9) :

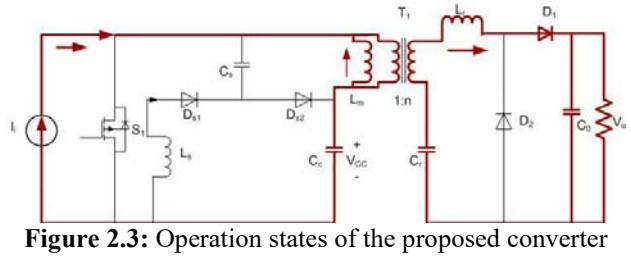

Figure 2.3: Operation states of the proposed converter

MODE 9 ($t_8 – t_9$) : Switch S_1 is in the turn-off state, and the sum of the input current and magnetizing current is being transferred to the secondary. Current i_{D1} is equal to $(I_i + I_{Lm})/n$. This mode ends when switch S_1 is turned ON.

3. Proposed Converter

The overall block diagram of the proposed converter is as shown in figure 3.1

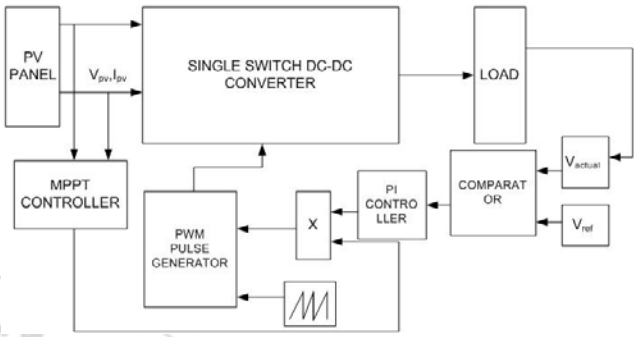

Figure 3.1: Block Diagram of proposed Converter

The input to the converter is fed from a PV panel whose efficiency can be improved using a suitable MPPT controller. Here efficiency of the PV panel is improved using Perturb & Observe algorithm. Inorder to maintain a constant output voltage irrespective of load and input variations a Voltage mode control is imparted in the proposed converter. In voltage mode control, there is a single voltage feedback path in which PWM is performed by comparing the error signal with a constant triangular waveform. In voltage mode control, the difference between the desired and actual output voltages controls the applied voltage across the filter inductor. Since voltage mode control needs to monitor the output voltage only one feedback path is required, thus simplifies the design of the converter.

4. PV Modeling

A simplest equivalent circuit of a solar cell is a current source in parallel with a diode. The output of the current source is directly proportional to the solar energy (photons) that hits on the solar cell (photocurrent I_{ph}). During darkness, the solar cell is not an active device; it works as a diode, i.e. a p-n junction. It produces neither a current nor a voltage. However, if it is allowed to connect to an external source (large voltage) it generates a current I_d, called diode (D) current or dark current. The diode determines the IV characteristics of the cell.

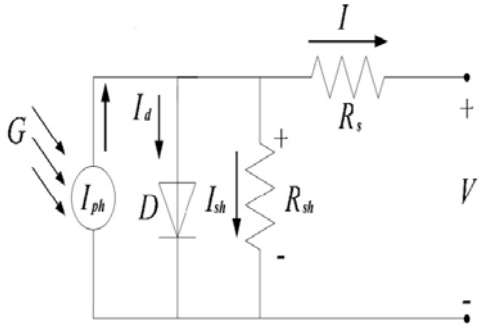

Figure 4.1: Circuit diagram of a PV cell

The circuit diagram of a PV cell is shown above in Fig 4.1. Accurate simulation is obtained after considering the following parameters:

- Temperature dependence of the diode reserved saturation current I_s.
- Temperature dependence of the photo current I_{ph}.
- Series resistance R_s(internal losses due to the current flow) which gives a more accurate shape between the maximum power point and the open circuit voltage.
- Shunt resistance R_{sh}, in parallel with the diode, this corresponds to the leakage current to the ground.

The voltage-current characteristics equation of a solar cell is given as

$$I = N_p I_{ph} - N_p I_s \left[\exp\left(\frac{q(V + IR_s)}{N_s k T_c A}\right) - 1\right]$$

Where, I_{ph} is a light-generated current or photo-current, I_s is the cell saturation of dark current, q(= 1.6 x 10^{-19} C) is an electron charge, k(= 1.38 x 10^{-23} J/K) is a Boltzmann's onstant, T_C is the cell's working temperature, A is an ideal factor, R_{sh} is shunt resistance,and R_s is a series resistance of solar cell.

C. Perturb & Observe MPPT Algorithm.

To improve the efficiency of the solar panel MPPT is used. According to maximum power point theorem, output power of any circuit can be maximize by adjusting source impedance equal to the load impedance, so the MPPT algorithm is equivalent to the problem of impedance matching.

In this paper Perturb and Observe (P&O) is used, because it require less hardware complexity and low-cost implementations.

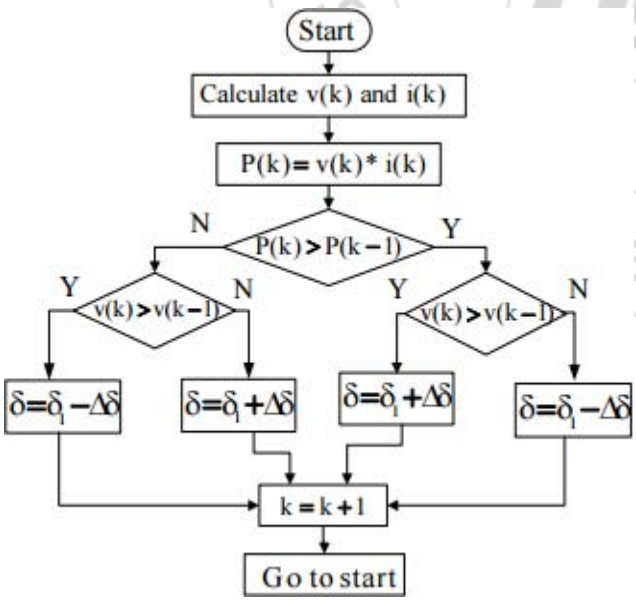

Figure 4.2: Flow chart of P&O MPPT Algorithm.

It is the simplest method of MPPT to implement. In this method only voltage is sensed, so it is easy to implement. In this method power output of system is checked by varying the supplied voltage. If on increasing the voltage, power is also increases then further ‚δ" is increased otherwise start decreasing the ‚δ'. Similarly, while decreasing voltage if power increases the duty cycle is decreased. These steps continue till maximum power point is reached. The corresponding voltage at which MPP is reached is known as reference point (V_{ref}). The entire process P&O algorithm is shown in Fig.4.2.

5. Simulation Results

The simulation of single switch soft switched isolated Boost DC-DC Converter has been carried out. An input voltage of 28V and switching frequency of 100 kHz is chosen and an output of 380V is obtained. The duty ratio is equal to 0.653 and the corresponding parameters are listed in Table 5.1.

Table 5.1: Component ratings

No	Components	Ratings
1	Filter inductor Li	100 μH
2	Snubber inductor Ls	5 μH
3	Snubber capacitor Cs	16 nF
4	Clamp capacitor Cc	82 μH
5	Resonant capacitor Cr	560 nF

a) Openloop Simulation results

Figure 5.1. Shows the open loop simulink model of the present converter.

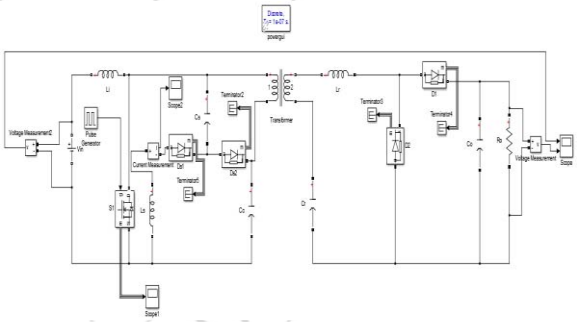

Figure 5.1: Simulink model of single switch ZVS-ZCS converter.

The input and output voltage waveforms of the converter is shown in figure 5.2. When an input voltage of 28V is given, the converter produces a high output voltage of 380V.

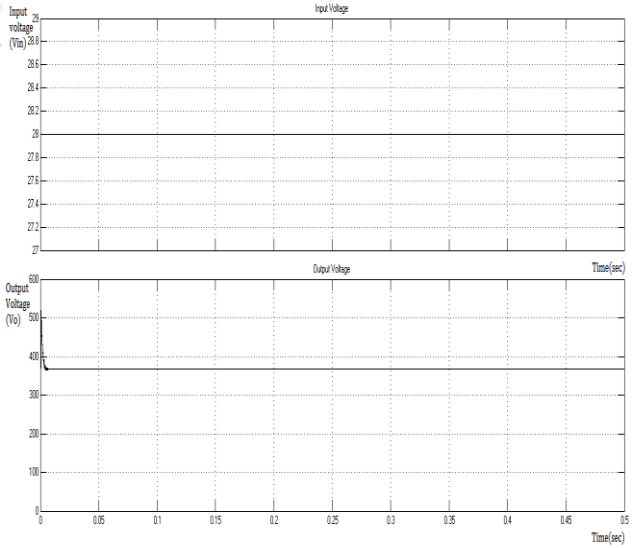

Figure 5.2: Input and output voltage waveforms

Figure 5.3 shows the gating pulse and ZVS-ZCS switching of the main switch S1.

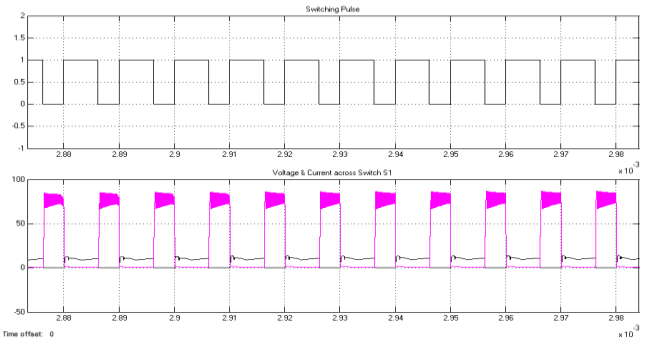

Figure 5.3: Gating pulse and ZVS-ZCS waveform across S1

b) Simulation of PV panel.

Figure 5.4 shows the Simulink model of the PV panel.

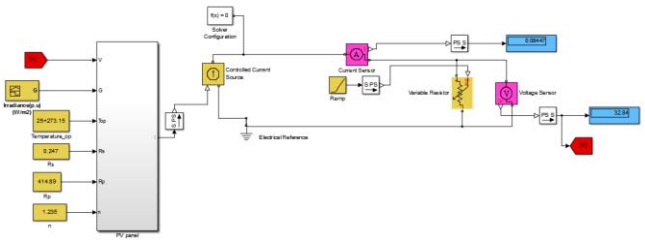

Figure 5.4: PV Simulink model.

The P-V and I-V characteristics of the photovoltaic panel for various solar insolation and at a temperature of 25°C is shown in (a) & (b).

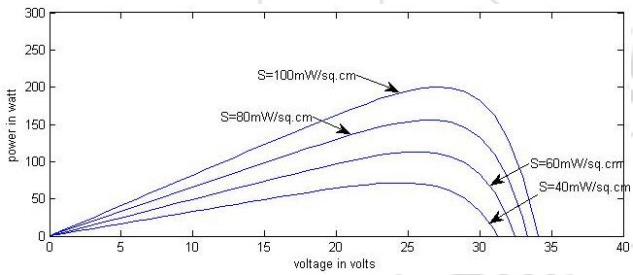

(a)

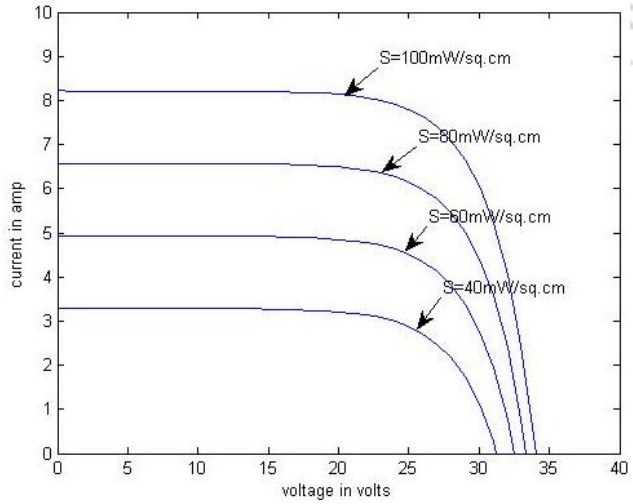

(b)

Figure 5.5: (a) P-V & (b) I-V curves for different insolations

The parameters that determine the operation of a photovoltaic panel is reflected in their characteristic curves, I-V and P-V. The current-voltage curves relations at various solar irradiations are obtained for photovoltaic panel working. For a radiation level between 400 - 1000 W/m^2, PV module output increases in the range 4 - 10%.

c) Closed loop simulation of Proposed converter

The overall Simulink model of the proposed converter with PV panel and voltage mode control is shown in figure 5.6.

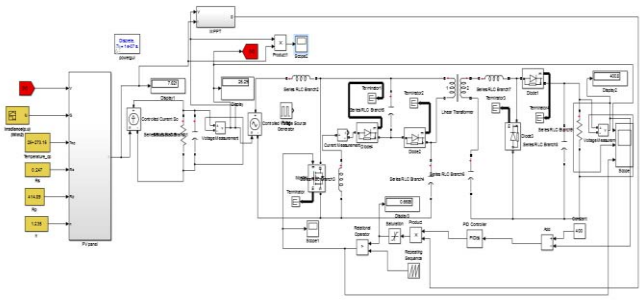

Figure 5.6: Closed loop Simulink model of PV fed single switch converter

Here, the actual input to the converter is fed from a PV panel whose efficiency is improved using MPPT controller. The voltage mode control using PI controller enables the output voltage to maintain constant irrespective of input and load variations. Figure 5.7 shows input and output voltage waveforms of the converter under closed loop control.

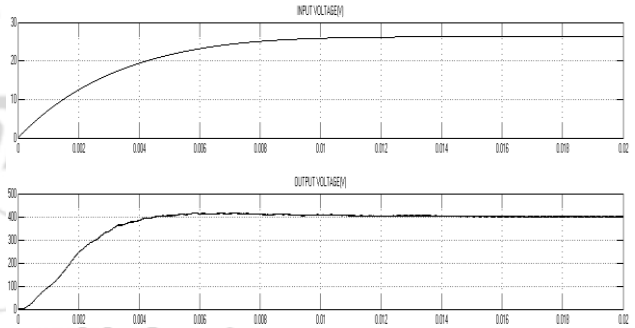

Figure 5.7: Input & Output voltage waveforms of the proposed converter

6. Conclusion

A PV fed single switch isolated converter is presented for step up applications. In the presented voltage mode control topology, the actual output voltage is compared to the desired output voltage and the difference (error) is used to adjust the PWM duty cycle to control the voltage across the inductor. Inorder to improve the efficiency of the PV panel P&O MPPT algorithm has been used. The main advantages of the converter includes 1) ZCS turn on and ZVS turn off of switch. 2) ZVS turn off of diodes regardless of voltage and load variations 3) Low rated lossless snubber is used for reducing magnetizing current. The presented voltage mode control helps the converter to maintain output voltage constant irrespective of change in PV output and load variations. Converter is validated through MATLAB simulations.

References

[1] Minjae Kim and Sewan Choi "A Fully Soft-Switched Single Switch Isolated DC–DC Converter" *IEEE transactions on power electronics*, vol. 30, no. 9, september 2015.
[2] M. Nymand and M. A. E. Andersen, "High-efficiency isolated boost DC-DC converter for high-power low-voltage fuel-cell applications," IEEETrans. Ind. Electron., vol. 57, no. 2, pp. 505–514, Feb. 2010.
[3] F. Evran and M. T. Aydemir, "Isolated high step-up DC-DC converter with low voltage stress," *IEEE Trans. Power Electron.*, vol. 29, no. 7, pp. 3591–3603, Jul. 2014.
[4] D. A. Ruiz-Caballero and I. Barbi, "A new flyback-current-fed push-pull DC-DC converter," *IEEE Trans. Power Electron.*, vol. 14, no. 6, pp. 1056– 1064, Nov. 1999.
[5] Park, En-Sung, et al. "A soft-switching active-clamp scheme for isolated full-bridge boost converter." *Proc. IEEE APEC*. Vol. 2. 2004
[6] A. Emrani, E. Adib, and H. Farzanehfard, "Single-switch soft-switched isolated DC-DC converter," *IEEE Trans. Power Electron.*, vol. 27, no. 4, pp. 1952–1957, Apr. 2012.
[7] J.M. Kwon,W.-Y. Choi, and B.-H. Kwon, "Single-switch quasi-resonant converter," *IEEE Trans. Ind. Electron.*, vol. 56, no. 4, pp. 1158–1163, Apr. 2009.
[8] J.H. Lee, J.-H. Park, and J. H. Jeon, "Series-connected forward-flyback converter for high step-up power conversion," *IEEE Trans. Power Electron.*, vol. 26, no. 12, pp. 3629–3641, Dec. 2011.
[9] Nema, S., Nema, R.K., Agnihotri, G., "Matlab simulink based study of photovoltaic cells/modules/array and their experimental verification",*International Journal of Energy and Environment*, vol.1(3), 2010, pp.487 - 500.
[10] Kanchan Ghute, Vinay kale, "A Simplied Matlab Based Simulation Of PV Module With Effect Of Temperature And Irradiation",*International Journal of Engineering and Technical Research (IJETR)*,vol.2, Issue-4, April 2014.
[11] G.Spiazzi, P. Mattavelli, and A. Costabeber, "High stepup ratio yback converter with active clamp and voltage multiplier", *IEEE Trans. Power Electron*., vol. 26, no. 11, pp. 3205 3214, Nov. 2011
[12] V. Yakushev, V. Meleshin, and S. Fraidlin, "Full-bridge isolated current fed converter with active clamp", *in Proc. IEEE Appl. Power Electron.Conf.*
[13] *Expo*., vol. 1, 1999, pp.560 - 566.
[14] S. Han, H. Yoon, G. Moon, M. Youn, Y. Kim, and K. Lee, "A new active clamping zero-voltage switching PWM current-fed half-bridge converter",
[15] *IEEE Trans. Power Electron*., vol. 20, no. 6, pp. 1271 - 1279, Nov. 2005.